Effect of Polymer Concentration on the Structure and Dynamics of Short Poly(N,N-dimethylaminoethyl methacrylate) in Aqueous Solution

Mintis, Dimitris G.; Dompe, Marco; Kamperman, Marleen; Mavrantzas, Vlasis G.

Published in:
Journal of Physical Chemistry B

DOI:
10.1021/acs.jpcb.9b08966

Publication date:
2020

THE JOURNAL OF PHYSICAL CHEMISTRY B

Article

Cite This: J. Phys. Chem. B 2020, 124, 240−252

pubs.acs.org/JPCB

Effect of Polymer Concentration on the Structure and Dynamics of Short Poly(*N*,*N*-dimethylaminoethyl methacrylate) in Aqueous Solution: A Combined Experimental and Molecular Dynamics Study

Dimitris G. Mintis,[†] Marco Dompé,[‡] Marleen Kamperman,[§] and Vlasis G. Mavrantzas*[,†,∥]

[†]Department of Chemical Engineering, University of Patras & FORTH-ICE/HT, GR 26504 Patras, Greece

[‡]Physical Chemistry and Soft Matter, Wageningen University, Stippeneng 4, 6708 WE Wageningen, The Netherlands

[§]Polymer Science, Zernike Institute for Advanced Materials, University of Groningen, Nijenborgh 4, 9747 AG Groningen, The Netherlands

[∥]Particle Technology Laboratory, Department of Mechanical and Process Engineering, ETH Zürich, CH-8092 Zürich, Switzerland

Supporting Information

ABSTRACT: A combined experimental and molecular dynamics (MD) study is performed to investigate the effect of polymer concentration on the zero shear rate viscosity η_0 of a salt-free aqueous solution of poly(*N*,*N*-dimethylaminoethyl methacrylate) (PDMAEMA), a flexible thermoresponsive weak polyelectrolyte with a bulky 3-methyl-1,1-diphenylpentyl unit as the terminal group. The study is carried out at room temperature (T = 298 K) with relatively short PDMAEMA chains (each containing N = 20 monomers or repeat units) at a fixed degree of ionization (α^+ = 100%). For the MD simulations, a thorough validation of several molecular mechanics force fields is first undertaken for assessing their capability to accurately reproduce the experimental observations and established theoretical laws. The generalized Amber force field in combination with the restrained electrostatic potential charge fitting method is eventually adopted. Three characteristic concentration regimes are considered: the dilute (from 5 to 10 wt %), the semidilute (from 10 to 20 wt %), and the concentrated (from 20 to 29 wt %); the latter two are characterized by polymer concentrations c_p higher than the characteristic overlap concentration c_p^*. The structural behavior of the PDMAEMA chains in the solution is assessed by calculating the square root of their mean-square radius of gyration $\langle R_g^2\rangle^{0.5}$, the square root of the average square chain end-to-end distance $\langle R_{ee}^2\rangle^{0.5}$, the ratio $\langle R_{ee}^2\rangle/\langle R_g^2\rangle$, and the persistence length L_p. It is observed that at low polymer concentrations, PDMAEMA chains adopt a stiffer and slightly extended conformation because of excluded-volume effects (a good solvent is considered in this study) and electrostatic repulsions within the polymer chains. As the polymer concentration increases above 20 wt %, the PDMAEMA chains adopt more flexible conformations, as the excluded-volume effects seize and the charge repulsion within the polymer chains subsides. The effect of total polymer concentration on PDMAEMA chain dynamics in the solution is assessed by calculating the orientational relaxation time τ_c of the chain, the center-of-mass diffusion coefficient D, and the zero shear rate viscosity η_0; the latter is also measured experimentally here and found to be in excellent agreement with the MD predictions.

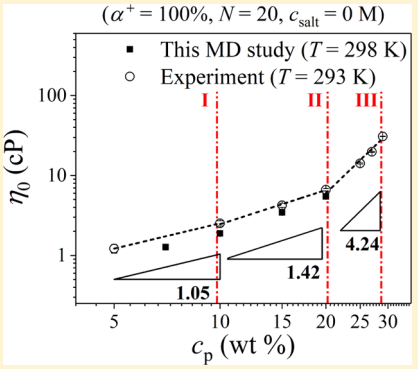

1. INTRODUCTION

Poly(*N*,*N*-dimethylaminoethyl methacrylate) (PDMAEMA) is a well-known water-soluble synthetic weak polyelectrolyte whose pH-responsiveness and thermoresponsiveness are attributed to the tertiary amine groups on the side chains along its backbone. Its versatile nature allows for conformational and dynamical variations upon changing the pH, the temperature, the ionic strength (salt concentration), the total polymer concentration, and the molecular weight. For this reason, it is used in a wide range of applications: as a viscosity adjusting agent in cosmetics,[1,2] as a solubility enhancer in food industry,[3,4] and as a drug delivery agent in medical industry.[5]

PDMAEMA has been thoroughly studied in the last years for its potential usage in the formation of complex coacervates resulting from the complexation of oppositely charged macromolecules as they undergo an associative liquid−liquid phase separation.[6] Thermoresponsive complex coacervate materials play a major role in the development of "high-performance" underwater adhesives because of a unique combination of properties such as immiscibility with water and good wetting of the surface.[7] During the last decade, polyelectrolytes have been greatly utilized in oil and gas industry as rheology modifiers for controlling and delaying gelation in the subterranean zone (a reaction zone of groundwater and seawater) in drilling and fracking processes.[8]

Received: September 20, 2019
Revised: December 6, 2019
Published: December 10, 2019

DOI: 10.1021/acs.jpcb.9b08966
J. Phys. Chem. B 2020, 124, 240−252

Surprisingly, there has been no work, neither experimental nor computational, addressing the dynamical behavior of PDMAEMA solutions with a short chain length ($N < 50$) and its dependence on polymer concentration. On the contrary, several previous noteworthy experimental studies[9,10] have addressed the rheological behavior of PDMAEMA solutions with considerably longer chain lengths ($N > 700$); they have shown that protonated PDMAEMA in solution behaves as a strong polyelectrolyte but adopts a flexible, coil-like conformation in the high-salt (NaCl) limit, both in the semidilute unentangled and entangled concentration regimes, implying a shift of its behavior toward that of a neutral polymer. The key element of the present work is the execution of both experiments and simulations in order to examine the dynamical as well as the structural behavior of short PDMAEMA chains ($N = 20$) when fully ionized (protonated) in salt-free solutions, as a function of total polymer concentration at room temperature ($T = 298$ K). Our interest in short PDMAEMA stems from the fact that similar chain length PDMAEMA chains have been studied experimentally[6,11,12] to determine the binodal composition of polyelectrolyte complexes of PDMAEMA with poly(acrylic acid) (PAA) of practically the same chain length. Our work here (as well as the recent one on the molecular dynamics (MD) simulation of aqueous solutions of short PAA chains[13]) is the first step toward predicting (at a given pH) the salt−polymer phase diagram for associative phase separation between PAA and PDMAEMA chains characterized by molecular lengths in the range between 20 and 50 repeat units (i.e., practically identical to those addressed experimentally) directly from the simulations at molecular level.

The dimensions of polymers in solutions depend significantly on the quality of the solvent and the total polymer concentration. Graessley[14] has classified polymer solutions into five different regimes: the dilute regime, the semidilute unentangled and entangled regimes, and the concentrated unentangled and entangled regimes. The distinction between the different regimes has been made based on the variation of chain dimensions in the solution with total polymer concentration and molecular weight. Unlike neutral polymers, the crossover from the dilute to the semidilute concentration regime for charged polymers (polyelectrolytes) occurs at lower concentrations. This is primarily attributed to the fact that charged polymers possess greater chain rigidity in solution than neutral polymers because of the electrostatic repulsion that arises between charges, which drastically affects the local flexibility and tends to increase the global dimensions of the chain.[15,16] Neutral polymers in a θ solvent retain a coil conformation,[17] whereas in a good solvent (in the dilute concentration regime), the coils are expanded because of the excluded-volume effect.[18] On the contrary, charged macromolecules behave as wormlike chains (WLCs), bridging the polymer behavior from coils to rigid rods.[19,20] For example, in a recent MD study, PAA, another weak polyelectrolyte, was found to adopt a WLC conformation when alternately or fully ionized.[13] Polyelectrolytes are classified as flexible, semiflexible, and rigid depending on local rigidity (persistence length of the backbone) and ionic strength (salt concentration).[21,22]

The crossover for WLCs from the dilute to the semidilute, and from the semidilute to the concentrated regime, has been well defined theoretically by Ying and Chu,[23] by incorporating two parameters: (a) the effective length $L^* = (L_pL_c)^{1/2}$, where L_p is the persistence length and L_c is the contour length of the polymer and (b) an effective diameter $d^* = d(L_c/L_p)^{1/4}$, where d is the diameter (thickness) of the macromolecule; in general, d^* is concentration-dependent, as the persistence length is also concentration-dependent (see also Results and Discussion section below). The critical overlap concentration of WLCs from a dilute to a semidilute solution is defined as $c_p^* = (2^{3/2}M)/(N_AL^{*3})$, where M is the molecular weight of the polymer and N_A denotes Avogadro's number, whereas the corresponding critical overlap concentration of WLCs from a semidilute to a concentrated solution is defined as $c_p^{**} = (0.243M)/(N_Ad^*L^{*2})$. In our study, a comprehensive analysis of the critical overlap concentration which distinguishes the dilute from the semidilute and the concentrated regimes is performed.

The dependence of the chain dimensions of flexible polyelectrolyte chains on the total polymer concentration has been described by several scaling theories in the past, as proposed by De Gennes et al.,[16] Pfeuty,[24] and Dobrynin and co-workers,[25] in which, however, the polymer persistence length and other parameters related to chain rigidity (stiffness) were not considered. In the present study, the global size of PDMAEMA chains in solution (only a good solvent is considered) is measured by estimating the square root $\langle R_g^2\rangle^{0.5}$ of the mean-squared radius of gyration and the square root $\langle R_{ee}^2\rangle^{0.5}$ of the mean-squared chain end-to-end distance, which for simplicity will be denoted in the following as R_g and R_{ee}, respectively. Dobrynin and co-workers[25] suggest that for salt-free polyelectrolytes in a good solvent, the value of R_{ee} in dilute solution has no dependence on the total polymer concentration; thus, $R_{ee} \approx c_p^0$; however, for $c_p > c_p^*$, a scaling behavior of the form $R_{ee} \approx c_p^{-1/4}$ is found. The obtained exponent of $-1/4$ is consistent with the study of De Gennes and co-workers[16] and should be contrasted with the corresponding exponent of $-1/8$ for neutral polymers.[17] A noteworthy study by Nierlich and co-workers[26] on the mean radius of gyration of a flexible polyelectrolyte with $N = 122$ in a salt-free solution by small-angle neutron scattering revealed that at a high polymer concentration R_g decreases as $c_p^{-1/4}$, whereas at a low polymer concentration, the ratio $R_g/R_{g,rod}$ (with $R_{g,rod}$ being the radius of gyration of the macromolecule if considered to be fully stretched) is around 0.87 and decreases as the polymer concentration increases. In addition, an MD study of a linear flexible polyelectrolyte chain modeled as a freely joined, bead-chain polymer with $N = 16$, 32, and 64 by Stevens and Kremer[27] revealed that the persistence length L_p decreases as the polymer concentration increases, thus suggesting that at low polymer concentrations the polyelectrolyte chain is stiffer than at high polymer concentrations. Stevens and Kremer[27] also reported that the ratio $\langle R_{ee}^2\rangle/\langle R_g^2\rangle$ at low polymer concentrations is between 8 and 10, implying a stiff coil conformation, but when the polymer concentration was increased, they found that $\langle R_{ee}^2\rangle/\langle R_g^2\rangle \cong 6$, indicating a change in chain conformation from being stretched to coiled (ideal chain).

The effect of polymer concentration on chain dimensions drastically affects the chain dynamics in the solution. Well-established theories have been proposed to describe this dynamics as a function of polymer concentration, such as the Zimm model for dilute solutions, the Rouse model for unentangled concentrated solutions, and the Doi−Edwards model for entangled concentrated solutions and melts.[17,28,29] Dobrynin et al.[25] and Muthukumar[30] found that the dynamics of linear flexible polyelectrolytes in the dilute concentration

DOI: 10.1021/acs.jpcb.9b08966
J. Phys. Chem. B 2020, 124, 240−252

Table 1. List of All Simulated Systems Conducted in This Work and Technical Details

no	N (mer)	c_p (wt %)	c_{salt} (M)	T (K)	force field	charge method	H_2O model	α^+ (%)	total simulation time (ns)
1	30		0	303	MMFF	MMFF	TIP4P/2005	50	70
2	30		0	338	MMFF	MMFF	TIP4P/2005	50	70
3	30		0	303	GAFF	RESP	TIP4P/2005	50	200
4	30		0	338	GAFF	RESP	TIP4P/2005	50	200
5	30		0	303	OPLS	RESP	TIP4P/2005	50	200
6	30		0	338	OPLS	RESP	TIP4P/2005	50	200
7	30		0	303	MMFF	RESP	TIP4P/2005	50	200
8	30		0	338	MMFF	RESP	TIP4P/2005	50	200
9	30		0	338	PCFF	PCFF	PCFF	50	120
10	20	5	0	298	GAFF	RESP	TIP4P/2005	100	1069
11	20	7	0	298	GAFF	RESP	TIP4P/2005	100	928
12	20	10	0	298	GAFF	RESP	TIP4P/2005	100	921
13	20	15	0	298	GAFF	RESP	TIP4P/2005	100	880
14	20	20	0	298	GAFF	RESP	TIP4P/2005	100	890
15	20	25	0	298	GAFF	RESP	TIP4P/2005	100	1002
16	20	29	0	298	GAFF	RESP	TIP4P/2005	100	1437

regime can be described by the Zimm model because of strong hydrodynamic interactions. The Zimm model has been found to be applicable in the case of the dynamics of a weak polyelectrolyte chain, PAA, at an infinite dilution based both on experimental[31] and MD[13] studies. According to Dobrynin and co-workers,[25] in the low-salt limit in the semidilute unentangled regime, the chain center-of-mass diffusion coefficient D is concentration-independent, whereas the zero shear rate viscosity η_0 grows with the square root of the concentration ($\eta_0 \approx c_p^{1/2}$), which agrees with the phenomenological law proposed by Fuoss.[32,33] In the high-salt semidilute unentangled regime, the dependence of the zero shear rate viscosity on polymer concentration is described as $\eta_0 \approx c_p^{5/4}$. In the case of the low-salt limit in the semidilute entangled regime, the zero shear rate viscosity scales as $\eta_0 \approx c_p^{3/2}$, whereas in the high-salt regime, above a certain concentration where the electrostatic blobs begin to overlap, the zero shear rate viscosity scales as $\eta_0 \approx c_p^{15/4}$ (i.e., the same as for uncharged polymers in a good solvent[25]). The diffusion coefficient D in the low-salt semidilute entangled regime scales with the total polymer concentration as $D \approx c_p^{-1/2}$ and as $D \approx c_p^{-7/4}$ in the high-salt regime. As described by the theoretical work of Dobrynin and co-workers,[25] the dependence of relaxation time τ_c on polymer concentration for polyelectrolyte solutions is predicted to decrease (it scales as $c_p^{-1/2}$) in the unentangled semidilute regime but to be independent of the polymer concentration in the entangled semidilute regime. There is still a lack of published theories on the dependency of the relaxation time on polyelectrolyte concentration in a salt-free solution in the dilute concentration regime. The experimental work of Wyatt and Liberatore[34] on the solution rheology of a flexible polyelectrolyte chain (xanthan gum with a molecular weight of 212 Da) revealed that the relaxation time τ_c in the dilute limit scales with the total polymer concentration as $\tau_c \approx c_p^{1.5}$, whereas in the limit above the characteristic concentration where electrostatic blobs begin to overlap as $\tau_c \approx c_p^{4}$.

To the best of our knowledge, only one MD simulation study[35] has addressed the behavior of PDMAEMA chains in solution. It employed the polymer consistent force field (PCFF),[36] but no comparison to experiment or theory was reported. In addition, relatively short simulation times were accessed, on the order of ∼30 ns. In the present work, we carry out a systematic analysis of several molecular mechanics force fields for the behavior of PDMAEMA in aqueous solution and examine in detail their validity and reliability to reproduce experimental observations and theoretical laws. Our study includes a thorough analysis of the critical overlap concentration c_p^* marking the crossover from the dilute to the semidilute concentration regime for PDMAEMA solutions with a fixed chain length of $N = 20$ at a fixed ionization state ($\alpha^+ = 100\%$) and temperature ($T = 298$ K). We address the scaling of chain size and flexibility with the polymer concentration, including predictions for the diffusion coefficient, the characteristic relaxation time, and the zero shear rate viscosity, and how they compare to the established theory and previous studies.

Being a thermoresponsive polymer, the effect of temperature on the chain dimensions of PDMAEMA would, of course, be of great importance. However, our main interest in this work is in the PDMAEMA properties at room temperature because it is only at this temperature that the equilibrium binodal composition between the polyelectrolyte complexes or coacervates of PDMAEMA and fluorescently labeled PAA with their coexisting dilute phases was measured by Spruijt et al.,[6,11,12] as a function of polymer chain length and salt concentration. However, we hope to carry out a systematic study of temperature effects on the conformation of short PDMAEMA chains in aqueous solution in the near future, in order to check how accurately the force field chosen here can describe the pH-dependence of the lower critical solution temperature (or even the upper critical solution temperature in the presence of multivalent counterions in aqueous solution) in comparison to the available experimental data in the literature.[37−41]

The rest of our work is organized as follows: Section 2 provides a brief description of the experiments carried out and of the systems simulated and the properties addressed. Section 3 presents a detailed discussion regarding force field validation and the effect of total polymer concentration on the structural and dynamical behavior of PDMAEMA in solution. Our paper concludes with Section 4 summarizing the most important findings of the present study and briefly highlighting possible future directions.

DOI: 10.1021/acs.jpcb.9b08966
J. Phys. Chem. B 2020, 124, 240−252

2. MATERIALS AND METHODS

2.1. Experiments. PDMAEMA with an atactic stereochemistry was purchased from Polymer Source, Inc. Its number average molecular weight M_n is 2.7 kg mol^{-1} (equivalent to a PDMAEMA chain with the degree of polymerization N = 20) and its polydispersity index is 1.16. The polymer was dissolved in Millipore water in concentrations spanning from 0 to 29 wt %. The pH of the solution was adjusted to 5.0.

Rheological measurements were performed on an Anton Paar MCR501 stress-controlled rheometer equipped with a Couette geometry (CC-17) with an outer diameter of 18.08 mm, a length of 25 mm, and a bob size of 16.66 mm. The solution was loaded in the rheometer at a temperature of 20 °C and then tetradecane was added above the solution to prevent water evaporation. The sample viscosity η was measured by performing rotation experiments at shear rates $\dot{\gamma}$ ranging from 100 to 0.01 s^{-1}. The torque T decreased as a function of the shear rate, and the lowest measurable value was 0.01 μN·m. For every concentration studied, the zero shear rate viscosity η_0 was obtained by averaging the values obtained at the lowest shear rates, where the Newtonian plateau was obtained, before reaching the minimum torque.

2.2. MD Simulations. Table 1 provides a list of all systems simulated in this work by MD together with the detailed information regarding technical aspects such as the molecular mechanics force field employed for PDMAEMA chains and water molecules, charge fitting method used, molecular length or number of monomers N of the simulated PDMAEMA chains, simulation temperature T (K), total polyelectrolyte concentration c_p (wt %), salt concentration c_{salt} (M), degree of PDMAEMA chain protonation α^+ (%), and total simulation time (ns).

The chemical structure of the protonated PDMAEMA molecules assumed in the MD study (relevant to the experimental chemical structure as reported by Polymer Source, Inc.) is presented in Figure 1. In all cases, atactic stereochemistry was adopted.

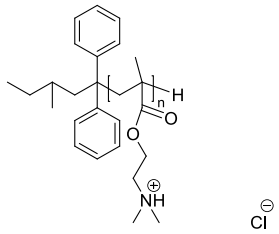

Figure 1. Chemical structure of the protonated PDMAEMA molecule.

In addition, and for the purpose of validating the accuracy of several molecular mechanics force fields on the basis of their comparison to the predictions made from a previous MD study,[35] the chemical structure (Figure 2) for the alternate protonated PDMAEMA molecule was adopted in order to be consistent with the chemical structure adopted in the previous study.

The MD simulations were performed using the GROMACS simulation package version 2016.3.[42−44] All initial configurations were built in the Materials and Processes Simulations (MAPS platform, version 4.2, Scienomics SARL, Paris, France) platform of Scienomics using a modified configurational bias

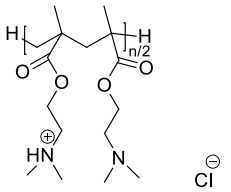

Figure 2. Chemical structure of the alternate protonated PDMAEMA molecule.

Monte Carlo scheme.[45,46] A cubic simulation cell with periodic boundary conditions applied in all directions was used for all systems. Sufficiently large cubic cells were constructed whose edge was larger than 2 times the mean end-to-end distance of PDMAEMA chains in order to prevent spurious interactions of the molecule with its periodic images in the neighboring cells. The same energy minimization and equilibration protocol was applied for all simulated systems. The initial configurations were energy-minimized by employing the steepest descent method to eliminate atomic overlaps, with the criterion for energy convergence set to 50 kJ mol^{-1} nm^{-1}. Next, a short simulation of 1 ns in the canonical (nVT) statistical ensemble was employed (n denotes the total number of interacting units in the simulation cell, V the volume of the cell, and T the temperature) with a time step of 1 fs for the integration of the equations of motion at the temperature of interest (see Table 1). The temperature was maintained constant by using a Nosé−Hoover thermostat with a coupling constant of 2.5 ps. Long MD production runs were next carried out in the isobaric−isothermal (nPT) statistical ensemble where P denotes the applied pressure (=1 bar), with a time step of 1 fs for the integration of the equations of motion. In this case, the Nosé−Hoover thermostat was combined with the Parrinello−Rahman barostat for the simultaneous control of temperature and pressure, with a coupling constant of 1 ps for both of them (see Table 1). In the simulations, the bond lengths and bond bending angles were assumed flexible. The particle mesh Ewald method[47] was used for computing the long-range electrostatic interactions.

The pH in our study was adjusted based on the protonation level of the PDMAEMA molecule. At acidic pH, the PDMAEMA molecule was assumed to be fully protonated (all nitrogen atoms were fully protonated); at neutral pH, on the other hand, the PDMAEMA molecule was assumed to be alternate protonated (alternate nitrogen atoms were protonated). The case of basic pH was not considered in our study. The TIP4P/2005 water model was used to solvate the PDMAEMA chains. Appropriate counterions (Cl^-) were added to ensure the electroneutrality of the system. Molecule topologies needed to describe the inter- and intramolecular interactions of the PDMAEMA chains were created based on four different force fields: (a) the generalized Amber force field (GAFF),[48] (b) the optimized potential for liquid simulations force field (OPLS),[49] (c) the Merck molecular force field (MMFF), and (d) the PCFF.[36] The GAFF and OPLS molecule topologies were obtained from the open source code ACPYPE,[50] the molecule topology for MMFF from the SwissParam[51] topology generation tool, and the molecule topology for PCFF from MAPS. The partial atomic charges were generated based on the restrained electrostatic potential (RESP)[52] method, with the input for the electronic densities provided from single-point energy calculations at the Hartree−Fock level of theory with the 6-31G* basis set. The quantum-

DOI: 10.1021/acs.jpcb.9b08966
J. Phys. Chem. B 2020, 124, 240−252

mechanical calculations for the computation of electronic densities were carried out with GAMESS-US[53,54] (version 2016R1). Section S1 of the Supporting Information provides a detailed description of the assigned atomic partial charges for the PDMAEMA molecule, for both pH cases considered (acidic and neutral).

The functional form of the total potential energy in the case of the GAFF force field is

$$E_{ij} = \frac{1}{2}\sum_{\text{bond}} k_{ij}^{\text{bonds}}(b_0 - b_{ij})^2 + \frac{1}{2}\sum_{\text{angles}} k_{ijk}^{\text{angle}}(\theta_0 - \theta_{ijk})^2 + \left(\sum_{\text{dihedrals}} k_{ijkl}^{\text{dihedral}}[1 + \cos(n\phi - \phi_s)] \text{ or } \sum_{n=0} C_n(\cos(\phi - 180))^n\right) + 4\sum \varepsilon_{ij}\left[\left(\frac{\sigma_{ij}}{r_{ij}}\right)^{12} - \left(\frac{\sigma_{ij}}{r_{ij}}\right)^{6}\right] + f\sum \frac{q_i q_j}{r_{ij}} \quad (1)$$

In eq 1, the first three terms denote the bonded contributions to the total potential energy from bond stretching, bond angle bending, and torsion angle twisting. The last two terms denote the additional intermolecular contributions to the total potential energy from van der Waals and electrostatic energies. The numerical values of all parameters in eq 1 are provided in Sections S1 and S2 of the Supporting Information.

2.3. Properties Calculated from the MD Simulations.

2.3.1. End-To-End Distance and Radius Of Gyration. To characterize the global shape of the PDMAEMA macromolecule in a solution, the square root $\langle R_{ee}^2\rangle^{0.5}$ of the mean-square end-to-end distance and the square root $\langle R_g^2\rangle^{0.5}$ of the mean-square radius of gyration were calculated as the statistical measures of the polymer's size, with the brackets denoting the averages over all possible PDMAEMA molecule configurations.

2.3.2. Persistence Length. To characterize the stiffness of the PDMAEMA molecule, the persistence length L_p was calculated. The persistence length is defined as the mean value of the projection of the end-to-end vector $\mathbf{R}_{ee}$ on the direction of the first bond $\mathbf{l}_1$ of the chain

$$L_p = \frac{\langle \mathbf{R}_{ee}\cdot\mathbf{l}_1\rangle}{|\mathbf{l}_1|} \quad (2)$$

and provides a measure of the number of main-chain bonds in a persistence segment.[17] We can actually generalize the above definition by considering in the place of $\mathbf{l}_1$ any bond $\mathbf{l}_i$ along the chain and then taking the average over all such bonds

$$L_p = \frac{1}{N_b}\sum_{i=1}^{N_b}\frac{\langle \mathbf{R}_{ee}\cdot\mathbf{l}_i\rangle}{|\mathbf{l}_i|} \quad (3)$$

where N_b is the total number of bonds along the chain. We expect this approach to provide a better measure of the intrinsic chain stiffness and thus of L_p.

For the freely rotating chain model developed and extensively described by Benoit,[55] Kratky and Porod,[56] and Flory[57] for which bond lengths and bond angles are assumed to be constant, equal to $|\mathbf{l}_n| = l_b$ and $\pi - \theta$, respectively, and bonds are allowed to rotate freely along the corresponding cone, it can be shown that[58]

$$L_p = l_b\frac{1 - (\cos\theta)^{N_b}}{1 - \cos\theta} \quad (4)$$

and

$$\langle R_{ee}^2\rangle = \left[\frac{1 + \cos\theta}{1 - \cos\theta} - 2\cos\theta\frac{1 - (\cos\theta)^{N_b}}{N_b(1 - \cos\theta)^2}\right]N_b l_b^2 \quad (5)$$

Clearly, in the limit of a very long chain ($N_b \gg 1$)

$$L_p = \frac{l_b}{1 - \cos\theta} \quad (6)$$

and

$$\langle R_{ee}^2\rangle = \frac{1 + \cos\theta}{1 - \cos\theta}N_b l_b^2 \quad (7)$$

Combining eqs 6 and 7, we get (for $N_b \gg 1$)

$$\langle R_{ee}^2\rangle = 2L_pL_c\left(1 - \frac{l_b}{2L_p}\right) \Rightarrow L_p = \frac{\langle R_{ee}^2\rangle}{2L_c} + \frac{l_b}{2} \quad (8)$$

where $L_c = N_b l_b$ denotes the contour length of the chain. In the case $l_b \ll L_p$, the freely rotating chain model predicts $\langle R_{ee}^2\rangle = 2L_pL_c$.

For the so-called continuously curved or WLC model, on the other hand, the persistence length can be calculated from the rate of decay of the bond−bond correlation function along the chain contour, namely

$$\langle \mathbf{l}_i\cdot\mathbf{l}_{i+n}\rangle = l_b^2\exp\left[-\frac{nl_b}{L_p}\right] \quad (9)$$

where $\mathbf{l}_i$ and $\mathbf{l}_{i+n}$ are bond vectors along the chain lying n bonds apart. In addition, one can prove that[17]

$$\langle R_{ee}^2\rangle = 2L_pL_c\left[1 - \frac{L_p}{L_c}(1 - e^{-L_c/L_p})\right] \quad (10)$$

which is the analogue of eq 8 of the freely rotating chain model. In the limit $L_p \ll L_c$, the WLC model predicts that $\langle R_{ee}^2\rangle = 2L_pL_c$, which agrees with the prediction of the freely rotating chain model in the limit $l_b \ll L_p$. On the other hand, in the limit $L_p/L_c \gg 1$, the WLC model predicts $\langle R_{ee}^2\rangle = L_c^2$, suggesting that the polymer displays a rigid rod behavior. The WLC model can therefore describe very different types of macromolecules.

2.3.3. Diffusion Coefficient. The calculation of the polymer's center-of-mass diffusion coefficient is achieved by using the Einstein relationship, namely $D = (1/6)\lim_{t\to\infty} d\langle|\mathbf{r}_i(t) - \mathbf{r}_i(0)|^2\rangle/dt$, where $\mathbf{r}_i(t)$ denotes the position of the i-th polymer's center of mass at time t and the angle brackets denote the mean-square displacement (msd) over all polymer's centers of mass. The diffusion coefficient is obtained in the Fickian regime where the slope of the log(msd)-versus-log(t) plot is equal to unity.

2.3.4. Viscosity. The zero shear viscosity is calculated by using the equilibrium method based on pressure fluctuations through the corresponding Green−Kubo (GK) relation, η_0 =

DOI: 10.1021/acs.jpcb.9b08966
J. Phys. Chem. B 2020, 124, 240−252

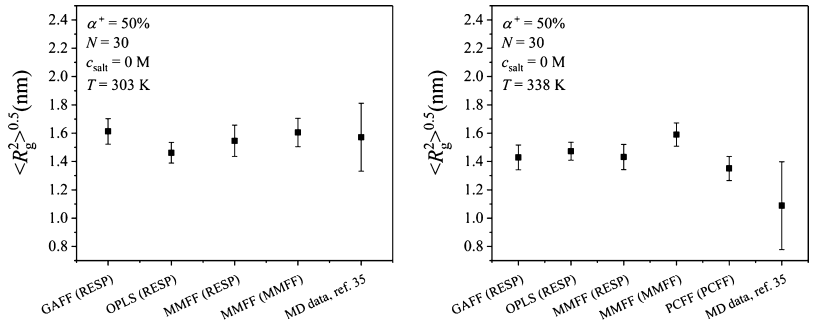

Figure 3. MD simulation predictions for R_g from the various molecular mechanics force fields and charge fitting techniques examined in this work and comparison with the previous MD study.[35]

$V/(k_BT)\int_0^\infty \langle P_{xz}(0)P_{xz}(t)\rangle dt$, where $P_{xz}(t)$ is the xz element of the pressure tensor at time t, and the angle brackets indicate an ensemble average. The integral is evaluated numerically, multiplied by $V/(k_BT)$, and averaged over the three off-diagonal components of the pressure tensor to estimate the viscosity.

3. RESULTS AND DISCUSSION

3.1. Force Field Validation. A systematic evaluation of several molecular mechanics force fields was carried out in this section to validate their capability in accurately and consistently predicting the conformational and dynamical behavior of the PDMAEMA chain in its solution, in comparison to a previous MD study,[35] previous experiments,[9,10] the new experiments carried out here, and the established theories.[17,25] The square root of the mean-square radius of gyration (denoted as R_g) is used as a measure to validate the conformational behavior of the PDMAEMA chain in the solution. The key advantage of R_g over the square root of the mean-square end-to-end distance (denoted as R_{ee}) and the persistence length L_p is that it accounts directly for the side-chain effects which are of particular importance for PDMAEMA, given that it contains considerably large side chains with chargeable carboxyl and amino groups.

Our validation analysis includes long MD simulations with the four different molecular mechanics force fields (GAFF, OPLS, MMFF, and PCFF) in combination with the atomic partial charges derived from the the RESP fitting method or MMFF charges. To model intra- and intermolecular interactions because of water molecules, the TIP4P/2005 water model is chosen, as it is found from several studies to predict more accurately the self-diffusion coefficient and the zero shear rate viscosity of water in comparison to experiments.[59−62] The time evolution of R_g from our MD simulations with the different molecular mechanics force fields examined is presented in Section S3 of the Supporting Information. In all cases, the MD results are obtained from very long simulation runs to ensure full convergence of the equilibrium value of R_g. Indeed, it takes about 100 ns for R_g to converge, which has to be contrasted with the total simulation time of 30 ns employed in the past.[35]

Figure 3 presents how the predicted R_g values obtained from the different molecular mechanics force fields compare with each other for a PDMAEMA chain with the degree of polymerization N = 30 and the degree of ionization α^+ = 50%, at two different temperatures (T = 303 and 338 K) in a salt-free aqueous solution. At T = 303 K, the R_g values from all of them compare very well (within the statistical error) with the R_g value obtained from the previous MD study.[35] However, at T = 338 K, the MMFF force field in combination with the partial atomic charges taken from MMFF overestimates slightly the value of R_g. We believe that the R_g value reported in the previous MD study[35] is considerably underestimated because of the short simulation run conducted in ref 35. By running the MD simulation for much longer times using the same molecular mechanics force field (PCFF) as the one reported by Min and co-workers,[35] the value of R_g obtained compares quite well, within the statistical error, with the value of R_g obtained from the other three force fields (GAFF, OPLS, and MMFF). The statistical errors reported in Figure 3 for the values retrieved from the previous MD study[35] are calculated by considering the fluctuations of R_g over the course of the simulation from 0 to 30 ns.

We next explore the accuracy and reliability of the GAFF force field to successfully predict the dynamical behavior of PDMAEMA in solution, in combination with the atomic partial charges derived from the RESP fitting method. This is accomplished by carrying out both MD simulations and experiments to study the zero shear rate viscosity of PDMAEMA solutions characterized by the fixed chain length (N = 20) and fixed degree of ionization (α^+ = 100%) at T = 298 K, as a function of total polymer concentration c_p (=5, 7, 10, 15, and 20 wt %). The results obtained are reported in Figure 4 and suggest that the zero shear rate viscosities obtained from this MD study compare qualitatively well with the experimentally measured values, with a small difference that can very well be attributed to the 5 °C difference between the experimental and simulated temperatures.

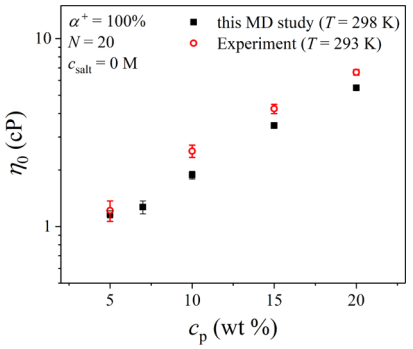

Figure 4. Comparison of simulation and experiment with regard to the zero shear rate viscosity of a PDMAEMA solution as a function of total polymer concentration.

DOI: 10.1021/acs.jpcb.9b08966
J. Phys. Chem. B 2020, 124, 240−252

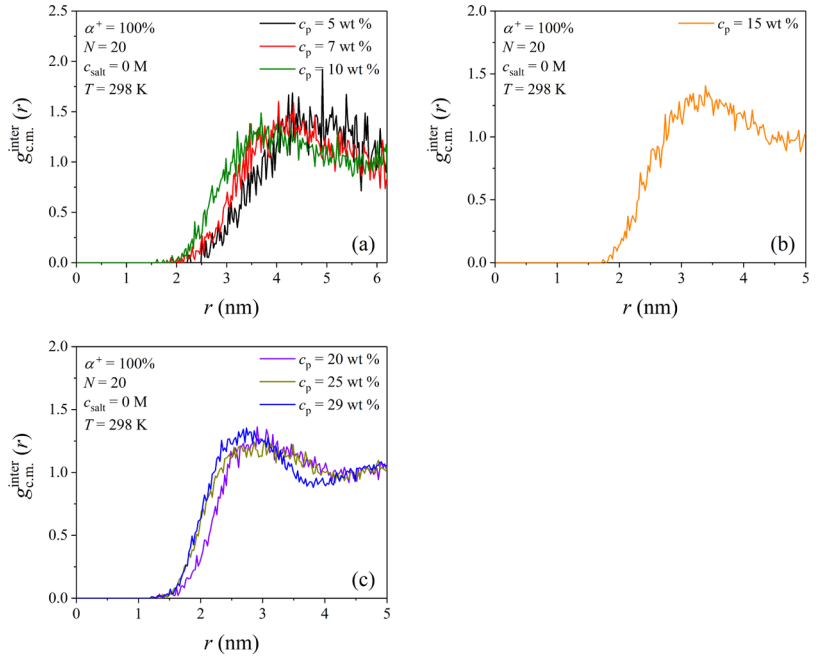

Figure 5. Intermolecular PDMAEMA chain center-of-mass radial pair distribution function in solution and dependence on total polymer concentration.

Based on our validation study, we decided to adopt the GAFF force field together with the atomic charges derived from the RESP fitting method to further analyze the conformational and dynamical behaviors of PDMAEMA chains in aqueous solution as a function of their total concentration.

3.2. Effect of Total Polymer Concentration. *3.2.1. Concentration Regimes.* Based on the formula proposed by Ying and Chu,[23] the critical overlap concentration c_p^* is estimated to be around c_p^* = 9.7 wt %. The second crossover concentration from the semidilute to the concentrated regime is found to be around c_p^{**} = 20.9 wt %. The two characteristic concentrations c_p^* and c_p^{**} can also be determined from our MD study by computing the concentration at which a pair of PDMAEMA chains has its centers of mass at a distance less than $2R_g$ (approximately less than 3 nm) apart. This is shown in Figure 5 presenting the PDMAEMA chain center-of-mass radial pair distribution function $g^{inter}_{c.m.}(r)$ in the solutions studied here, as a function of total polymer concentration. According to Figure 5, PDMAEMA chains start overlapping strongly when their concentration in the solution is above 10 wt % (see Figure 5a,b). At this concentration, a significant number of PDMAEMA pairs appear to have their centers of mass at a distance less than 3 nm apart. The critical overlap concentration estimated from the MD simulations is therefore $c_p^* \approx 10$ wt % (or, equivalently, 0.097 g mL^{-1}). On the other hand, the system containing 20 wt % PDMAEMA is found to have a significant number of PDMAEMA pairs at distances between 1.5 and 2 nm (see Figure 5c), denoting the crossover from the semidilute to the concentrated regime; thus, according to our MD simulations, $c_p^{**} \approx 20$ wt % (which is approximately equivalent to 0.209 g mL^{-1}). In the literature, the volume fraction of the polymer at c_p^{**} is typically between 0.2 and 0.3 g mL^{-1}.[63] Our findings are in perfect agreement with the theoretical predictions based on the formula proposed by Ying and Chu.[23] As far as the system containing 15 wt % PDMAEMA is concerned, this has several pairs at distances between 2 and 3 nm apart; thus, this system is clearly in the semidilute regime. Overall, and for the rest of our study here, we distinguish three regimes as far as the dependence of the various physical properties of the simulated PDMAEMA solutions on concentration is concerned:

- Concentrations below 10 wt % corresponding to the dilute regime
- Concentrations between 10 and 20 wt % corresponding to the semidilute regime, and
- Concentrations above 20 wt % corresponding to the concentrated regime.

As only one system belongs clearly to the semidilute regime (the 15 wt % one), the unentangled and entangled regimes cannot be distinguished; so, the semidilute concentration regime is considered as a single regime. We further note that the initiator (the molecule required to control the living anionic polymerization of PDMAEMA) might also affect the concentration dependence of the structural and dynamical behavior of PDMAEMA in solution, as it introduces a bulky 3-methyl-1,1-diphenylpentyl unit as the terminal group.

Typical atomistic snapshots of PDMAEMA chains from our MD simulations in the three different concentration regimes with the systems considered in this work are depicted in Figure 6. In a recent all-atom MD study[64] on the effect of total polymer concentration and degree of ionization on the structure of atactic PAA chains with the chain length of N = 30 in a good solvent, it was observed that when $c_p \cong c_p^{**}$, local aggregates comprising few PAA chains are formed when the degree of ionization is equal to 20, 40, and 70%. In contrast, for fully ionized chains, no aggregate formation was observed. A similar observation is made here (see Figure 6): fully ionized PDMAEMA chains with the chain length of N = 20 do not form aggregates in solutions with $c_p > c_p^{**}$. As also discussed by Gupta and Natarajan,[64] repulsive interactions between chains are far more important than hydrophobic attractions; as a result, at high values of charge density, interchain aggregation of flexible chains is disfavored.

DOI: 10.1021/acs.jpcb.9b08966
J. Phys. Chem. B 2020, 124, 240−252

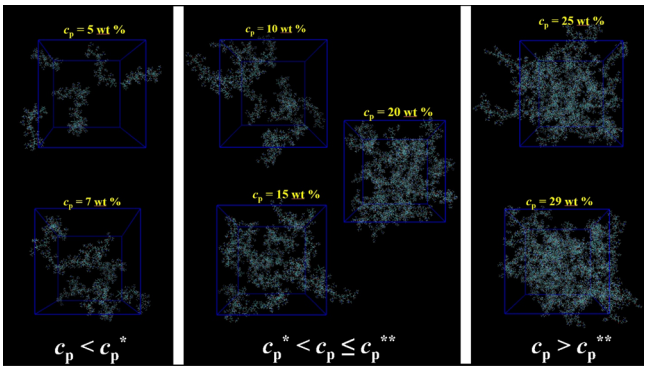

Figure 6. Representative atomistic snapshots of PDMAEMA chains in the three different concentration regimes for the systems considered in this work.

The ratio $\langle R_{ee}^2\rangle/\langle R_g^2\rangle$ (see Figure 8) approaches within statistical error the value of 6.3, which is very close to the value

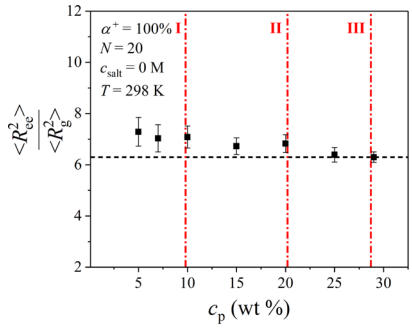

Figure 8. Concentration dependence of $\langle R_{ee}^2\rangle/\langle R_g^2\rangle$. The black short dashed line denotes the ideal value, which is around 6.3 for flexible chain conformations in a good solvent.[27]

3.2.2. Conformational Properties and Chain Rigidity. We turn now to the effect of total polymer concentration c_p (=5, 7, 10, 15, 20, 25, and 29 wt %) on the conformational properties of PDMAEMA chains in solution (only the case of good solvent is considered). Figure 7 shows how R_g and R_{ee} vary with c_p. The graphs with the corresponding instantaneous values of R_g and R_{ee} are reported in Section S4 of the Supporting Information. In the dilute and semidilute regimes (5−20 wt %), the data shown in Figure 7a,b indicate only a very weak dependence of R_g and R_{ee} on c_p; in contrast, as the polymer concentration increases above 20 wt %, both R_g and R_{ee} exhibit a rather strong dependence on c_p, $R_g \approx c_p^{-0.10}$, and $R_{ee} \approx c_p^{-0.18}$. At a low polymer concentration, PDMAEMA chains remain swollen because of the excluded-volume effect which arises from the quality of the solvent employed (good solvent), but as the polymer concentration increases, they shrink, as the excluded-volume effect becomes negligible. The concentration dependence of the size of a polymer chain as a function of solvent quality is described quite well theoretically by the blob model.[63] Notably, Liao and co-workers[65] observed by means of MD simulation with several polyelectrolyte solutions that the exponent quantifying the power-law dependence of R_g or R_{ee} on c_p is N-dependent. For a fully charged polyelectrolyte chain and $c_p > c_p^*$, they reported that $R_{ee} \approx c_p^{-0.10}$ for N = 25, and $R_{ee} \approx c_p^{-0.22}$ for N = 300. Their results revealed that, for the longest chains (N = 187 and N = 300) simulated, the concentration dependence of R_g approaches the power law $c_p^{-1/4}$ predicted by the scaling model for salt-free polyelectrolytes.

of 6 characterizing Gaussian (i.e., random coil) polymer chains. This indicates that PDMAEMA chains tend to become Gaussian as the polymer concentration increases above 20 wt %. The short dashed line in the figure presents the value for flexible chains in a good solvent[27] which is around 6.3 (for ideal, random-walk chains, this value is around 6). According to the blob model, above the critical overlap concentration, blobs do not feel the excluded volume by the other blobs; thus, a chain of blobs assumes the conformation of an ideal chain.[63] Stevens and Kremer[27] report that the ratio $\langle R_{ee}^2\rangle/\langle R_g^2\rangle$ is N-dependent for $c_p < c_p^*$, but for $c_p > c_p^*$ the ratio becomes N-independent and approaches (within statistical error) the value for flexible chains in a good solvent (≈6.3). They also report that this ratio is around 7.9 for charged polyelectrolytes with the chain length N = 16 and around 10.2 for polyelectrolytes with the chain length N = 130 in dilute solutions. Their findings are in very good agreement with ours according to which PDMAEMA chains adopt a random coil conformation when their concentration in the aqueous solution increases above 20 wt %. In addition, the observation made in this study for the ratio $\langle R_{ee}^2\rangle/\langle R_g^2\rangle$ in a dilute solution agrees with our previous work,[13] wherein the ratio $\langle R_{ee}^2\rangle/\langle R_g^2\rangle$ for fully charged PAA chains with the chain lengths N = 20 and N = 23 was predicted to be around 8. The concentration dependence of $\langle R_{ee}^2\rangle/\langle R_g^2\rangle$ observed in this study is in very good agreement also with the small-angle neutron scattering data of Nierlich et al.,[26] according to which the ratio $R_g/R_{g,rod}$ of a polyion in salt-free solutions is around 0.87 in the low-concentration regime (where the polyion is very extended but

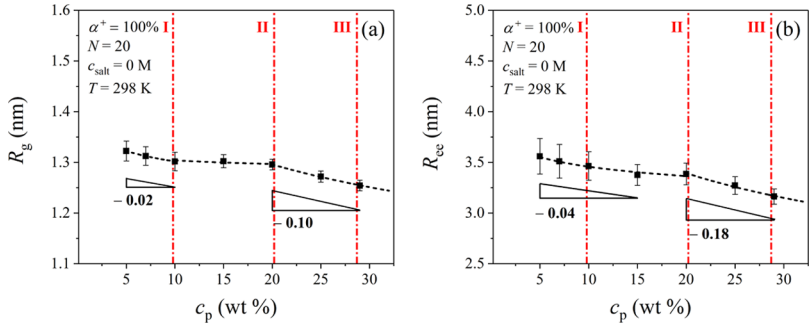

Figure 7. Concentration dependence of (a) R_g and (b) R_{ee}. The short dash-dotted red vertical lines are used to separate the three characteristic concentration regimes (I: dilute, II: semidilute, and III: concentrated).

DOI: 10.1021/acs.jpcb.9b08966
J. Phys. Chem. B 2020, 124, 240−252

not totally stretched) but decreases in the high-concentration regime.

The polymer concentration dependence of the chain rigidity (flexibility) of PDMAEMA solutions is examined by measuring the persistence length L_p. The simulation data are shown in Figure 10 and indicate that L_p decreases as the polymer concentration increases, thus suggesting that at low polymer concentrations the PDMAEMA chains obtain a stiffer conformation but at high concentrations they become more flexible. That the rigidity of PDMAEMA chains is considerably higher at low concentrations can be explained by two factors: the excluded-volume effect and the electrostatic repulsion that arises between charges within the chain. L_p scales with c_p as $L_p \approx c_p^{-0.09}$ in the dilute regime and as $L_p \approx c_p^{-0.31}$ for c_p above 20 wt %.

Table 1 in Section S5 of the Supporting Information presents the mean value of L_p for each one of the simulated systems, as computed from all the four different methods discussed above: (a) from eq 3 which utilizes all bonds along a PDMAEMA chain (see Figure 9), (b) from eq 8 which makes

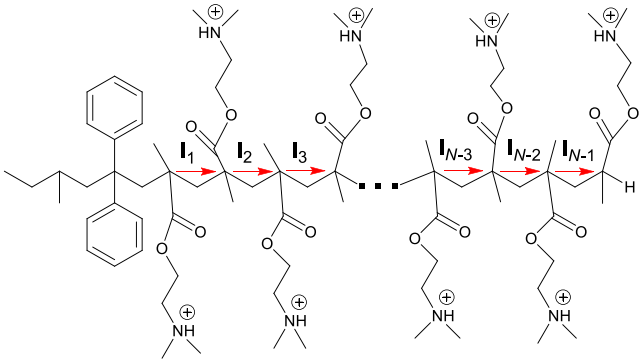

Figure 9. Schematic representation of the various bond vectors along a PDMAEMA chain used in the calculation of L_p.

use of the result of the mean-square chain end-to-end distance of the polymer, (c) from eq 9 which also utilizes all bonds along the chain, and (d) from eq 10 which, like eq 8, makes use of the result of the mean-square chain end-to-end distance of the polymer. Although the numerical values obtained are not identical, their differences are very small; the results are also consistent as far as the concentration dependence of L_p is concerned. This latter dependence is shown in Figure 10 where the L_p values plotted have been obtained from eq 9; we

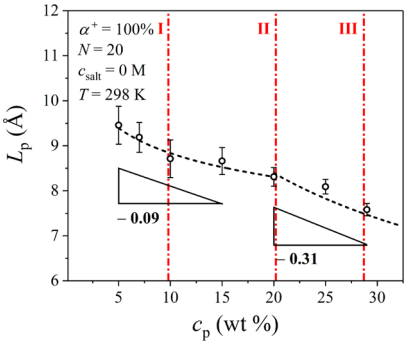

Figure 10. MD simulation results for the concentration dependence of L_p. As explained in the text, the values of L_p have been computed using eq 9.

see that L_p decreases monotonically with c_p. The concentration dependence of L_p found in our study agrees with the observations made in a previous MD study,[27] where it was observed that for a charged polyelectrolyte with the chain length N = 32, $L_p \approx c_p^{-0.08}$ for $c_p < c_p^*$ and $L_p \approx c_p^{-0.32}$ for $c_p > c_p^*$. For long charged polyelectrolytes (chain length N = 300), Liao and co-workers[65] report that $L_p \approx c_p^{-0.5}$ above the critical overlap concentration.

3.2.3. Relaxation Time. Figure 11 presents the decay of the time autocorrelation function $C(t)$ of the unit vector directed

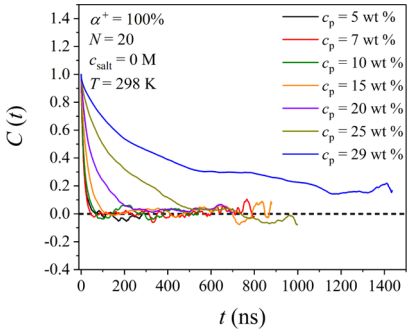

Figure 11. Time autocorrelation function of the chain end-to-end unit vector as a function of total polymer concentration c_p.

along the PDMAEMA chain end-to-end distance for the systems studied in this work. The rate with which this function drops to zero is a measure of the overall relaxation rate of the chain, and to compute it, rather long MD runs are needed because the long-length scale features of the polymer must have fully relaxed by the end of the simulation. The $C(t)$-versus-t plots shown in Figure 11 confirm that the structural relaxation of the chain depends strongly on the variations in the total polymer concentration.

From the MD-computed $C(t)$-versus-t curves, one can obtain the corresponding orientational relaxation time τ_c of the chain by fitting the $C(t)$-versus-t curve with a stretched exponential or KWW function of the form $\exp(-(t/\tau_{KWW})^{\beta})$, where τ_{KWW} is the characteristic time and β is the stretching exponent, and then using $\tau_c = \tau_{KWW}((\Gamma(1/\beta))/\beta)$. The dependence of τ_c on the total polymer concentration c_p is presented in Figure 12. Three regions of dependence between τ_c and c_p can be discerned in the figure. Between 5 and 10 wt %, no significant concentration dependence is seen. However, as the concentration increases first to 15 wt % and then to 20 wt %, a dramatic dependence is presented, which becomes

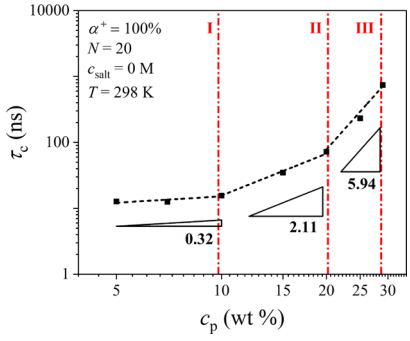

Figure 12. Log–log plot of the dependence of chain orientational relaxation time τ_c on the total polymer concentration c_p.

DOI: 10.1021/acs.jpcb.9b08966
J. Phys. Chem. B 2020, 124, 240−252

even more pronounced by further increasing c_p. To quantify the strong dependence of τ_c on c_p, we fitted the τ_c-versus-c_p data to a power law of the form $\tau_c \approx c_p^{\nu}$ and extracted the value of the exponent ν. The following data were obtained: $\nu = 0.32$ for c_p between 5 and 10 wt %, $\nu = 2.11$ for c_p between 15 and 20 wt %, and $\nu = 5.94$ for c_p between 20 and 29 wt %. In contrast to the weak concentration dependence of the conformational properties discussed in the previous section, the dynamics of PDMAEMA chains in their solution is drastically affected by their total concentration.

As it is noted by Doi and Edwards,[29] the topological constraints for linear polymers in many-chain systems do not dramatically affect the structure of the polymer, as all configurations are accessible; however, the topological constraints drastically affect the dynamics of the polymer by acting as obstacles to the motion of the chains. Above the critical overlap concentration c_p^*, in particular, chain dynamics is severely restricted by topological constraints because of other chains. According to Figure 12, as the polymer concentration increases above c_p^*, the value of τ_c rises steeply; above 20 wt %, in particular, a sharp increase is observed denoting the crossover from the semidilute to the concentrated regime. Strong topological constraints in this case render the dynamics of PDMAEMA solutions similar to the dynamics of a neutral polymer in the corresponding crowded background environment. We also recall (as already discussed above) that the scaling theories formulated to describe the structural and dynamical behavior of flexible polyelectrolytes in solution do not account for the polymer persistence length or other characteristics related to chain rigidity or the nature of side groups or branches along the polymer. The presence of the terminal bulky 3-methyl-1,1-diphenylpentyl unit in the PDMAEMA chains simulated here might also contribute to the observed behavior.

3.2.4. Diffusion Coefficient. The concentration dependence of the PDMAEMA chain center-of-mass diffusion coefficient D in the solution is obtained by means of the Einstein relationship (Section 2.3). Similar to the calculation of τ_c, long MD runs are again needed to ensure that the chain motion has reached the Fickian regime where the corresponding msd grows linearly with time (see Section S6.1 in the Supporting Information). Through such long MD runs, we obtained the PDMAEMA diffusivities shown in Figure 13 as a function of PDMAEMA concentration in the solution. The corresponding statistical errors were estimated based on the variation of the local slope of msd with respect to time (see Section S6.2 in the Supporting Information). By fitting the MD results for the dependence of D on c_p to a power law of the form $D \approx c_p^{\nu}$ (see Figure 13), three regions of dependence were revealed, consistent with the corresponding findings from the analysis of the concentration dependence of τ_c: (a) in the dilute regime between 5 and 10 wt %, D is practically concentration-independent (considering also the corresponding statistical error at each concentration); (b) as the total polymer concentration increases progressively to 15 wt % and then to 20 wt %, the values of D drop suddenly, following the scaling $D \approx c_p^{-1.42}$; (c) finally, in the regime between 20 and 29 wt %, D scales with c_p as $D \approx c_p^{-6.05}$, indicating the drastic increase of friction between the strongly overlapping, neighboring chains. Note also that the value of the exponent predicted in the semidilute regime (≈1.42) is considerably larger than the one suggested from theory (≈1/2 in the low-salt limit and ≈7/4 in the high-salt limit),[25] which can be attributed to the relatively short molecular length of PDMAEMA considered here as well as to the presence of the bulky terminal group.

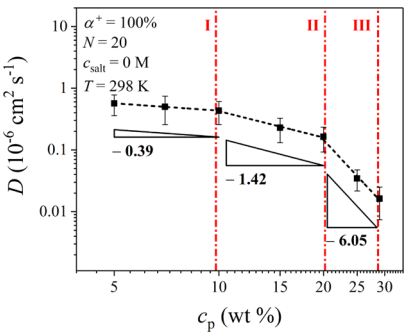

Figure 13. PDMAEMA chain center-of-mass diffusion coefficient D vs total polymer concentration c_p, as calculated from the present MD simulations. The three vertical red dash-dotted lines are used to separate the three characteristic concentration regimes (dilute, semidilute, and concentrated).

3.2.5. Shear Viscosity. The polymer concentration dependence of the zero shear rate viscosity η_0 of the PDMAEMA solutions simulated here ($N = 20$) is investigated by carrying out a thorough experimental and simulation study. First, experimental measurements of η_0 are obtained for solutions with $c_p = 5$, 10, 15, 20, 25, 27, and 29 wt % at temperature $T = 293$ K and zero salt concentration. To this, for each concentration, two samples were prepared, and viscosity measurements were collected for each sample. Figure 14a presents the measured viscosity-versus-shear rate data averaged over the two samples prepared for each concentration studied. Only the Newtonian plateau (corresponding to the zero shear rate viscosity) for the shear rates in the range between 1.0 and 0.01 s^{-1} is shown. Figure 14b, on the other hand, presents the zero shear viscosity as calculated from the MD simulations (at temperature $T = 298$ K) and how it compares with the corresponding experimental data for the various polymer concentrations studied. The MD viscosity values are determined by applying the GK formalism (see Section 2.3), following the time decomposition approach proposed by Zhang and co-workers.[66] Multiple independent trajectories (approximately 30) are employed for each concentration, and the GK relation is applied to each trajectory. Notably, the initial configurations of each trajectory are obtained from the equilibrated part of the production MD runs. Section S7 of the Supporting Information presents the average running integral of the GK formalism as a function of time, which is fitted to a double-exponential function with a weighting function derived from the standard deviation of the running integrals. As it is reported by Zhang and co-workers,[66] the formal GK integral requires an integration to infinite time, whereas an integration cutoff time t_{cut} could be determined by the relative values of the running integral and the corresponding standard deviation. Section S8 of the Supporting Information presents the sensitivity of the computed viscosity values to the number of trajectories used, until convergence of the averaged running integral is reached. As it is observed, 25−30 trajectories are enough for the averaged running integral of the GK relation to converge. MD trajectories on the order of 1−2 ns are performed to ensure no effect of trajectory length.

DOI: 10.1021/acs.jpcb.9b08966
J. Phys. Chem. B 2020, 124, 240−252

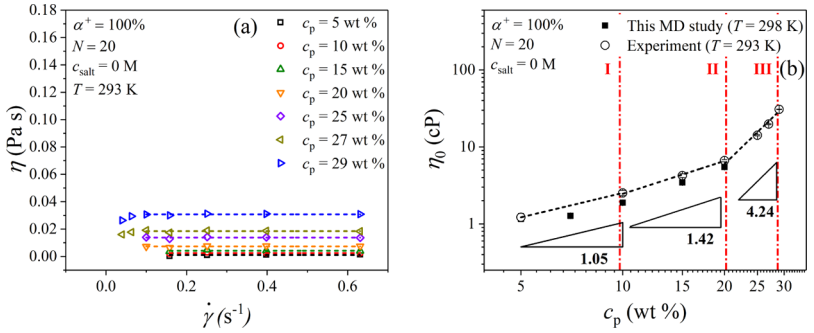

Figure 14. Plots of (a) shear viscosity as obtained experimentally vs applied shear rate and (b) zero shear rate viscosity vs total polymer concentration as calculated from experiment and simulation. The three characteristic concentration regimes discussed are defined by the three vertical red dash-dotted lines.

The zero shear rate viscosity as obtained experimentally scales with the polymer concentration as $\eta_0 \approx c_p^{\nu}$, with $\nu = 1.05$ in the range between 5 and 10 wt %, $\nu = 1.42$ in the range between 10 and 20 wt %, and $\nu = 4.24$ in the range between 20 and 29 wt %. These findings are in good agreement with a previous rheological experimental study[9] of PDMAEMA with $M_n = 113\,000$ g mol^{-1} (degree of polymerization $N = 719$) at pH = 5, according to which $\nu = 0.8$ and 1.7 in the unentangled and entangled semidilute regimes, respectively. The large scaling factor ($\nu = 4.24$) observed between 20 and 29 wt % in our experiments suggests that the dynamics of short PDMAEMA solutions is drastically disturbed in this concentration regime, revealing a crossover from the polyelectrolyte behavior to a random coil, neutral polymer behavior. This could be explained by the fact that, with increasing concentration, the electrostatic charges are screened out because of the overlap of electrostatic blobs; as a result, charge repulsion within polymer chains is hindered and the chains adopt a coil-like conformation. The concentration dependence of the rheological behavior of the PDMAEMA solutions is consistent with the corresponding observations made from the calculations of the chain center-of-mass diffusion coefficient D and relaxation time τ_c.

4. CONCLUSIONS

Surprisingly, only one MD simulation work has been carried out so far on the effect of pH and temperature on the solvation and structural behavior of PDMAEMA in aqueous media. Based on this, one of the key outcomes of the present study is the systematic investigation of the capability of several molecular mechanics force fields to reliably describe the conformational and dynamical properties of PDMAEMA in solution in comparison to the available experiment data and the previous MD study. The GAFF force field in combination with the RESP charge fitting method is found to provide the most accurate predictions in comparison to the previous MD study and previous experimental data, as well as to new experiments performed in this work.

Three characteristic concentration regimes are found: (a) the dilute (between 5 and 10 wt %), (b) the semidilute (between 10 and 20 wt %), and (c) the concentrated (between 20 and 29 wt %). The corresponding critical concentrations c_p^* and c_p^{**} denoting the passage from one to the other are found to be at 10 and 20 wt %, respectively, which is fully consistent with the theoretical predictions.

The effect of total polymer concentration on the structure of PDMAEMA chains in solution is investigated by means of long MD simulations through the calculations of several statistical measures, such as the mean radius of gyration R_g, the average end-to-end distance R_{ee}, the persistence length L_p, and the ratio $\langle R_{ee}^2 \rangle / \langle R_g^2 \rangle$. The latter, in dilute solution, is found to be around 6.5 and 8 implying that PDMAEMA obtains a stiff coil conformation, and as the polymer concentration increases above 20 wt %, it drops to around 6.3 which is close to the value for ideal flexible chains in a good solvent. No significant concentration dependence of the three statistical conformational measures is found in the dilute solution, but as the polymer concentration increases above 20 wt %, the following scalings are found: $R_g \approx c_p^{-0.10}$, $R_{ee} \approx c_p^{-0.18}$, and $L_p \approx c_p^{-0.31}$. This denotes a crossover in the conformational behavior of PDMAEMA with concentration, which can be attributed to the fact that PDMAEMA chains are swollen at low enough concentrations because of the excluded-volume effect (only good solvent is considered), but this effect gradually ceases as the concentration of the polymer in the solution increases. Our findings are consistent with previous studies and already established theories.

Regarding the concentration dependence of the dynamics of PDMAEMA, the chain orientational relaxation time τ_c, the chain center-of-mass diffusion coefficient D, and the solution zero shear rate viscosity η_0 are calculated. Experiments are also performed to assess the dependence of η_0 on the polymer concentration c_p. We find that τ_c and D show no dependence on c_p in the range between 5 and 10 wt % (dilute regime). In the range between 10 and 20 wt % (semidilute regime), τ_c and D scale with c_p as $\tau_c \approx c_p^{2.11}$ and $D \approx c_p^{-1.42}$, whereas in the range between 20 and 29 wt % (concentrated regime), $\tau_c \approx c_p^{5.94}$ and $D \approx c_p^{-6.05}$. The zero shear rate viscosity as calculated from the experiment and MD is found to be in very good agreement. According to the experimental data, the viscosity scales with c_p as $\eta_0 \approx c_p^{1.05}$ in the range between 5 and 10 wt % and as $\eta_0 \approx c_p^{1.32}$ in the range between 10 and 20 wt %. Above 20 wt %, the viscosity increases rapidly with the polyelectrolyte concentration, following the law $\eta_0 \approx c_p^{4.24}$; this suggests a crossover from the polyelectrolyte behavior to a random coil-like neutral polymer behavior.

Our study suggests that a short-chain length ($N = 20$), fully ionized, PDMAEMA with a bulky 3-methyl-1,1-diphenylpentyl unit as the terminal group behaves as a strong polyelectrolyte in the dilute and semidilute concentration regimes. This agrees perfectly with previous experimental studies[9,10] where it was suggested that protonated PDMAEMA chains with a considerably larger chain length ($N > 700$) behave as strong polyelectrolytes in the semidilute unentangled and entangled

DOI: 10.1021/acs.jpcb.9b08966
J. Phys. Chem. B 2020, 124, 240−252

concentration regimes. At concentrations around 20 wt %, the electrostatic blobs begin to overlap and thus the PDMAEMA chains behave as uncharged (neutral) polymers in solution. In the future, we intend to study more systematically the semidilute concentration regime in order to classify the dynamical and structural behavior of PDMAEMA solutions in the crossover regime from unentangled to entangled.

■ ASSOCIATED CONTENT

Supporting Information

The Supporting Information is available free of charge at https://pubs.acs.org/doi/10.1021/acs.jpcb.9b08966.

Coulomb partial charges as derived from the RESP charge fitting method for the completely ionized and alternate ionized PDMAEMA chain; inter- and intramolecular interactions and the values of parameters assigned to each atom in a PDMAEMA chain based on the GAFF molecular mechanics force field; time evolution of R_g and R_{ee} as obtained from the different molecular mechanics force fields implemented and tested in our work; time evolution of R_g and R_{ee} for all PDMAEMA solutions studied in this work as a function of total polymer concentration; mean value of L_p calculated by using five different methods; variation of the PDMAEMA chain center-of-mass msd with time and its instantaneous slope for all systems studied in this work; plots regarding the calculated averaged running integral of the GK equation and the corresponding standard deviation; effect of the number of independent trajectories on the viscosity calculated by the GK method (PDF)

■ AUTHOR INFORMATION

Corresponding Author

*E-mail: vlasis@chemeng.upatras.gr, vlasiosm@mat.ethz.ch. Phone: +30 6944 60 25 80, +41 44 632 8503.

ORCID

Marleen Kamperman: 0000-0002-0520-4534

Vlasis G. Mavrantzas: 0000-0003-3599-0676

Author Contributions

This manuscript was written by D.G.M. and V.G.M. with feedback from M.D. and M.K. All authors have given approval to the final version of the manuscript.

Notes

The authors declare no competing financial interest.

■ ACKNOWLEDGMENTS

The authors gratefully acknowledge full financial funding received from the European Union's Horizon 2020 research and innovation programme under the Marie Skłodowska-Curie grant agreement no. 642861 in the context of the BioSmartTrainee European Project. The work was supported by computational time granted from the Greek Research & Technology Network (GRNET) in the National HPC facility−−ARIS under project pr006011. To this, we further feel indebted to Dr. Ioannis Liabotis and Dr. Dimitrios Ntelis from GR-NET, Greece, for their support on several technical aspects of the work.

■ REFERENCES

(1) Liu, J.-F.; Min, G.; Ducker, W. A. AFM Study of Adsorption of Cationic Surfactants and Cationic Polyelectrolytes at the Silica−Water Interface. *Langmuir* **2001**, *17*, 4895−4903.

(2) Koetz, J.; Kosmella, S. *Polyelectrolytes and Nanoparticles*; Springer: Berlin, 2007.

(3) Schmitt, C.; Turgeon, S. L. Protein/polysaccharide complexes and coacervates in food systems. *Adv. Colloid Interface Sci.* **2011**, *167*, 63−70.

(4) Kadajji, V. G.; Betageri, G. V. Water soluble polymers for pharmaceutical applications. *Polymers* **2011**, *3*, 1972−2009.

(5) Cherng, J.-Y.; Van de Wetering, P.; Talsma, H.; Crommelin, D. J. A.; Hennink, W. E. Effect of size and serum proteins on transfection efficiency of poly ((2-dimethylamino) ethyl methacrylate)-plasmid nanoparticles. *Pharm. Res.* **1996**, *13*, 1038−1042.

(6) Spruijt, E.; Westphal, A. H.; Borst, J. W.; Cohen Stuart, M. A.; van der Gucht, J. Binodal Compositions of Polyelectrolyte Complexes. *Macromolecules* **2010**, *43*, 6476−6484.

(7) Dompé, M.; Cedano-Serrano, F. J.; Heckert, O.; van den Heuvel, N.; van der Gucht, J.; Tran, Y.; Hourdet, D.; Creton, C.; Kamperman, M. Thermoresponsive Complex Coacervate-Based Underwater Adhesive. *Adv. Mater.* **2019**, *31*, 1808179.

(8) Visakh, P. Polyelectrolytes: Thermodynamics and rheology. *Polyelectrolytes*; Springer: London, 2014.

(9) Hunley, M. T.; England, J. P.; Long, T. E. Influence of Counteranion on the Thermal and Solution Behavior of Poly(2-(dimethylamino)ethyl methacrylate)-Based Polyelectrolytes. *Macromolecules* **2010**, *43*, 9998−10005.

(10) McKee, M. G.; Hunley, M. T.; Layman, J. M.; Long, T. E. Solution rheological behavior and electrospinning of cationic polyelectrolytes. *Macromolecules* **2006**, *39*, 575−583.

(11) Spruijt, E.; Cohen Stuart, M. A.; van der Gucht, J. Linear viscoelasticity of polyelectrolyte complex coacervates. *Macromolecules* **2013**, *46*, 1633−1641.

(12) Spruijt, E.; Leermakers, F. A. M.; Fokkink, R.; Schweins, R.; van Well, A. A.; Cohen Stuart, M. A.; van der Gucht, J. Structure and dynamics of polyelectrolyte complex coacervates studied by scattering of neutrons, x-rays, and light. *Macromolecules* **2013**, *46*, 4596−4605.

(13) Mintis, D. G.; Mavrantzas, V. G. Effect of pH and molecular length on the structure and dynamics of short poly(acrylic acid) in dilute solution: Detailed molecular dynamics study. *J. Phys. Chem. B* **2019**, *123*, 4204−4219.

(14) Graessley, W. Polymer chain dimensions and the dependence of viscoelastic properties on concentration, molecular weight and solvent power. *Polymer* **1980**, *21*, 258−262.

(15) Fixman, M. The flexibility of polyelectrolyte molecules. *J. Chem. Phys.* **1982**, *76*, 6346−6353.

(16) De Gennes, P. G.; Pincus, P.; Velasco, R. M.; Brochard, F. Remarks on polyelectrolyte conformation. *J. Phys.* **1976**, *37*, 1461−1473.

(17) Rubinstein, M.; Colby, R. H. *Polymer Physics*; Oxford University Press: New York, 2003.

(18) Yamakawa, H. *Modern Theory of Polymer Solutions*; Harper & Row: New York, 1971.

(19) Skolnick, J.; Fixman, M. Electrostatic persistence length of a wormlike polyelectrolyte. *Macromolecules* **1977**, *10*, 944−948.

(20) Li, H.; Witten, T. A. Fluctuations and persistence length of charged flexible polymers. *Macromolecules* **1995**, *28*, 5921−5927.

(21) Jeon, J.; Chun, M.-S. Structure of flexible and semiflexible polyelectrolyte chains in confined spaces of slit micro/nanochannels. *J. Chem. Phys.* **2007**, *126*, 154904.

(22) Waigh, T. A. *The Physics of Living Processes: A Mesoscopic Approach*; John Wiley & Sons: Chichester, 2014.

(23) Ying, Q.; Chu, B. Overlap concentration of macromolecules in solution. *Macromolecules* **1987**, *20*, 362−366.

(24) Pfeuty, P. Conformation des polyelectrolytes ordre dans les solutions de polyelectrolytes. *J. Phys., Colloq.* **1978**, *39*, C2-149−C2-160.

DOI: 10.1021/acs.jpcb.9b08966
J. Phys. Chem. B 2020, 124, 240−252

(25) Dobrynin, A. V.; Colby, R. H.; Rubinstein, M. Scaling theory of polyelectrolyte solutions. *Macromolecules* **1995**, *28*, 1859−1871.
(26) Nierlich, M.; Boué, F.; Lapp, A.; Oberthur, R. Radius of gyration of a polyion in salt free polyelectrolyte solutions measured by SANS. *J. Phys.* **1985**, *46*, 649−655.
(27) Stevens, M. J.; Kremer, K. The nature of flexible linear polyelectrolytes in salt free solution: A molecular dynamics study. *J. Chem. Phys.* **1995**, *103*, 1669−1690.
(28) Heo, Y.; Larson, R. G. The scaling of zero-shear viscosities of semidilute polymer solutions with concentration. *J. Rheol.* **2005**, *49*, 1117−1128.
(29) Doi, M.; Edwards, S. F. *The Theory of Polymer Dynamics*; Oxford University Press: New York, 1986.
(30) Muthukumar, M. Dynamics of polyelectrolyte solutions. *J. Chem. Phys.* **1997**, *107*, 2619−2635.
(31) Dolce, C.; Mériguet, G. Ionization of short weak polyelectrolytes: When size matters. *Colloid Polym. Sci.* **2017**, *295*, 279−287.
(32) Fuoss, R. M. Viscosity function for polyelectrolytes. *J. Polym. Sci.* **1948**, *3*, 603−604.
(33) Rabin, Y.; Cohen, J.; Priel, Z. Viscosity of polyelectrolyte solutions-the generalized fuoss law. *J. Polym. Sci., Polym. Lett. Ed.* **1988**, *26*, 397−399.
(34) Wyatt, N. B.; Liberatore, M. W. Rheology and viscosity scaling of the polyelectrolyte xanthan gum. *J. Appl. Polym. Sci.* **2009**, *114*, 4076−4084.
(35) Min, S. H.; Kwak, S. K.; Kim, B.-S. Atomistic simulation for coil-to-globule transition of poly(2-dimethylaminoethyl methacrylate). *Soft Matter* **2015**, *11*, 2423−2433.
(36) Sun, H.; Mumby, S. J.; Maple, J. R.; Hagler, A. T. An ab initio cff93 all-atom force field for polycarbonates. *J. Am. Chem. Soc.* **1994**, *116*, 2978−2987.
(37) Plamper, F. A.; Ruppel, M.; Schmalz, A.; Borisov, O.; Ballauff, M.; Müller, A. H. E. Tuning the thermoresponsive properties of weak polyelectrolytes: Aqueous solutions of star-shaped and linear poly(n,n-dimethylaminoethyl methacrylate). *Macromolecules* **2007**, *40*, 8361−8366.
(38) Fournier, D.; Hoogenboom, R.; Thijs, H. M. L.; Paulus, R. M.; Schubert, U. S. Tunable pH- and Temperature-Sensitive Copolymer Libraries by Reversible Addition−Fragmentation Chain Transfer Copolymerizations of Methacrylates. *Macromolecules* **2007**, *40*, 915−920.
(39) Han, X.; Zhang, X.; Zhu, H.; Yin, Q.; Liu, H.; Hu, Y. Effect of composition of pdmaema-b-paa block copolymers on their pH- and temperature-responsive behaviors. *Langmuir* **2013**, *29*, 1024−1034.
(40) Plamper, F. A.; Ballauff, M.; Müller, A. H. E.; Muller, A. H. E. Tuning the thermoresponsiveness of weak polyelectrolytes by pH and light: Lower and upper critical-solution temperature of poly(n,n-dimethylaminoethyl methacrylate). *J. Am. Chem. Soc.* **2007**, *129*, 14538−14539.
(41) Bütün, V.; Armes, S. P.; Billingham, N. C. Synthesis and aqueous solution properties of near-monodisperse tertiary amine methacrylate homopolymers and diblock copolymers. *Polymer* **2001**, *42*, 5993−6008.
(42) Berendsen, H. J. C.; van der Spoel, D.; van Drunen, R. Gromacs: A message-passing parallel molecular dynamics implementation. *Comput. Phys. Commun.* **1995**, *91*, 43−56.
(43) Van Der Spoel, D.; Lindahl, E.; Hess, B.; Groenhof, G.; Mark, A. E.; Berendsen, H. J. C. Gromacs: Fast, flexible, and free. *J. Comput. Chem.* **2005**, *26*, 1701−1718.
(44) Abraham, M. J.; Murtola, T.; Schulz, R.; Páll, S.; Smith, J. C.; Hess, B.; Lindahl, E. Gromacs: High performance molecular simulations through multi-level parallelism from laptops to supercomputers. *SoftwareX* **2015**, *1−2*, 19−25.
(45) Theodorou, D. N.; Suter, U. W. Atomistic modeling of mechanical properties of polymeric glasses. *Macromolecules* **1986**, *19*, 139−154.
(46) Ramos, J.; Peristeras, L. D.; Theodorou, D. N. Monte carlo simulation of short chain branched polyolefins in the molten state. *Macromolecules* **2007**, *40*, 9640−9650.
(47) Darden, T.; York, D.; Pedersen, L. Particle mesh Ewald: An N·log(N) method for Ewald sums in large systems. *J. Chem. Phys.* **1993**, *98*, 10089−10092.
(48) Wang, J.; Wolf, R. M.; Caldwell, J. W.; Kollman, P. A.; Case, D. A. Development and testing of a general amber force field. *J. Comput. Chem.* **2004**, *25*, 1157−1174.
(49) Jorgensen, W. L.; Maxwell, D. S.; Tirado-Rives, J. Development and testing of the opls all-atom force field on conformational energetics and properties of organic liquids. *J. Am. Chem. Soc.* **1996**, *118*, 11225−11236.
(50) da Silva, A. W. S.; Vranken, W. F. ACPYPE - AnteChamber PYthon Parser interfacE. *BMC Res. Notes* **2012**, *5*, 367.
(51) Zoete, V.; Cuendet, M. A.; Grosdidier, A.; Michielin, O. Swissparam: A fast force field generation tool for small organic molecules. *J. Comput. Chem.* **2011**, *32*, 2359−2368.
(52) Bayly, C. I.; Cieplak, P.; Cornell, W.; Kollman, P. A. A well-behaved electrostatic potential based method using charge restraints for deriving atomic charges: the RESP model. *J. Phys. Chem.* **1993**, *97*, 10269−10280.
(53) Gordon, M. S.; Schmidt, M. W. Chapter 41 - Advances in electronic structure theory: Gamess a decade later. *Theory and Applications of Computational Chemistry*; Elsevier: Amsterdam, 2005; pp 1167−1189.
(54) Schmidt, M. W.; Baldridge, K. K.; Boatz, J. A.; Elbert, S. T.; Gordon, M. S.; Jensen, J. H.; Koseki, S.; Matsunaga, N.; Nguyen, K. A.; Su, S.; Windus, T. L.; Dupuis, M.; Montgomery, J. A. General atomic and molecular electronic structure system. *J. Comput. Chem.* **1993**, *14*, 1347−1363.
(55) Benoit, H. Calcul de l'écart quadratique moyen entre les extrémités de diverses chaînes moléculaires de type usuel. *J. Polym. Sci.* **2003**, *3*, 376−388.
(56) Kratky, O.; Porod, G. Röntgenuntersuchung gelöster fadenmoleküle. *Recl. Trav. Chim. Pays-Bas* **2010**, *68*, 1106−1122.
(57) Flory, P. J. *Statistical Mechanics of Chain Molecules*; Interscience Publishers: New York, 1969.
(58) Kroon-Batenburg, L. M. J.; Kruiskamp, P. H.; Vliegenthart, J. F. G.; Kroon, J. Estimation of the persistence length of polymers by MD simulations on small fragments in solution. Application to cellulose. *J. Phys. Chem. B* **1997**, *101*, 8454−8459.
(59) Tazi, S.; Boţan, A.; Salanne, M.; Marry, V.; Turq, P.; Rotenberg, B. Diffusion coefficient and shear viscosity of rigid water models. *J. Phys.: Condens. Matter* **2012**, *24*, 284117.
(60) Markesteijn, A. P.; Hartkamp, R.; Luding, S.; Westerweel, J. A comparison of the value of viscosity for several water models using Poiseuille flow in a nano-channel. *J. Chem. Phys.* **2012**, *136*, 134104.
(61) Guevara-Carrion, G.; Vrabec, J.; Hasse, H. Prediction of self-diffusion coefficient and shear viscosity of water and its binary mixtures with methanol and ethanol by molecular simulation. *J. Chem. Phys.* **2011**, *134*, 074508.
(62) González, M. A.; Abascal, J. L. F. The shear viscosity of rigid water models. *J. Chem. Phys.* **2010**, *132*, 096101.
(63) Teraoka, A. A.; Teraoka, I. *Polymer Solutions: An Introduction to Physical Properties*; John Wiley & Sons: New York, 2002.
(64) Gupta, A. K.; Natarajan, U. Structure and dynamics of atactic Na^+-poly(acrylic) acid (PAA) polyelectrolyte in aqueous solution in dilute, semi-dilute and concentrated regimes. *Mol. Simul.* **2019**, *45*, 876−895.
(65) Liao, Q.; Dobrynin, A. V.; Rubinstein, M. Molecular dynamics simulations of polyelectrolyte solutions: Nonuniform stretching of chains and scaling behavior. *Macromolecules* **2003**, *36*, 3386−3398.
(66) Zhang, Y.; Otani, A.; Maginn, E. J. Reliable viscosity calculation from equilibrium molecular dynamics simulations: A time decomposition method. *J. Chem. Theory Comput.* **2015**, *11*, 3537−3546.

DOI: 10.1021/acs.jpcb.9b08966
J. Phys. Chem. B 2020, 124, 240−252